Moving Target at Constant Velocity Localization Using TOA Measurements from Single Moving Receiver with Unknown Signal Period

Yanbin Zou, *Member, IEEE,* Jingna Fan, and Zekai Zhang

***Abstract*—In this paper, we consider using time-of-arrival (TOA) measurements from a single moving receiver to locate a moving target at constant velocity that emits a periodic signal with unknown signal period. First, we give the TOA measurement model and deduce the Cramér-Rao lower bounds (CRLB). Then, we formulate a nonlinear least squares (NLS) problem to estimate the unknown parameters. We use semidefinite programming (SDP) techniques to relax the nonconvex NLS problem. However, it is shown that the SDP localization algorithm cannot provide a high-quality solution. Subsequently, we develop a fixed point iteration (FPI) method to improve the performance of the SDP algorithm. In addition, we also consider the presence of receiver position errors and develop the corresponding localization algorithm. Numerical simulations are conducted to demonstrate the localization performance of the proposed algorithms by comparing them with the CRLB.**

***Index Term*-Fixed point iteration (FPI), semidefinite programming (SDP), single moving receiver, target localization, time-of-arrival (TOA).**

I. Introduction

TARGET localization has received tremendous interest in many fields, such as radar, sonar, wireless communication, and sensor networks [1]–[4].

Modern wireless localization systems often use several spatially separated receivers to cooperatively locate the source. Commonly used measurement parameters include time of arrival (TOA), time-difference of arrival (TDOA), angle of arrival (AOA), received signal strength (RSS), frequency-difference of arrival (FDOA), and their combinations [5]–[7]. The TOA and TDOA systems require timing synchronization between the spatially separated receivers [8] and need at least three receivers to locate the target. The AOA systems typically use an antenna array for direction estimation and also need at least two receivers to locate the target [9]. Compared to the multiple platform localization system, a single moving platform localization system has the merit of fast deployment, and data communication between platforms is also exempt [10]–[13].

Using a single moving receiver to locate a stationary emitter (referring to the position of the emitter is fixed in the process of localization) with bearing-only measurements, Doppler-only measurements, or a combination of bearing and Doppler measurements has been well studied in the literature [14]–[17]. Recently, TOA-based localization with a single moving receiver has also received a great deal of attention [18]–[22]. In [18], Tzoreff *et al.* developed a localization method for stationary emitters by using TOA measurements, in which the emitter transmits a periodic signal. It is assumed that the waveform and period are known to the receiver, then the periodicity is exploited to relate consecutive interceptions of the signal that occur at different locations. In other words, the signal periodicity compensates for the absence of simultaneous measurements collected by multiple sensors, and the localization problem will be equivalent to asynchronous TOA or TDOA localization [23], [24].

In [21], the authors investigated a new problem in which the signal period is unknown and the existence of missed detections of signal emissions is also considered. The authors proposed a two-step localization algorithm for the problem. In its first step, the signal propagation delay is ignored, and some existing period estimation techniques are used to roughly identify the period. In the second step, using an iterative method to jointly estimate the source position and the signal period. In [22], Zou *et al.* proposed a semidefinite programming (SDP)-based algorithm to jointly estimate source position and the period. Then, the SDP-based algorithm is extended to the presence of receiver position uncertainties. In [13], Feng *et al.* developed a 1-D search approach to estimate the target position, which has low computational complexity compared with the SDP-based algorithm in [22].

A drawback with the above mentioned works is that they are not applicable to the case of moving target. In [19], Madadi *et al.* extended the work in [18] by considering that the target is also moving. And the authors proposed an extended Kalman filter (EKF) to estimate the local oscillator (LO) offset, skew, target position, and speed simultaneously. However, it still assumes that the signal period is known. In the case of non-cooperative target localization, the signal period is usually unknown and also needs to be estimated.

In this paper, we consider using TOA measurements from a single moving receiver to locate a moving target with unknown signal period, which has not been studied so far. It is assumed that the target is moving at constant velocity, which is a common pattern in practice [19], [25]. It is worth noting that when the receiver receivers signals from more than one target, some off-the-shelf methods can be used to solved the problem of pulse match and signal separation [26]–[28], and then multiple targets localization can be processed separately. In the problem of localization a moving target at constant velocity using TOA measurements from a single moving receiver, the unknown parameters include start transmission time, signal period, target position at start transmission time, and target

The authors are with the Department of Electronic and Information Engineering, Shantou University, Shantou, Guangdong, 515063, China (e-mail: ybzou@stu.edu.cn).

This article has been accepted for publication in IEEE Open Journal of Signal Processing. This is the author's version which has not been fully edited and content may change prior to final publication. Citation information: DOI 10.1109/OJSP.2023.3338111

velocity. We formulate the localization problem as a nonlinear least-square (NLS) problem, but it is highly nonlinear and nonconvex, which leads to a closed-form solution is hard to obtain.

The main contributions of this paper are as follows:

- This is the first effort, to the best of our knowledge, to develop a TOA-based moving target at constant velocity localization model using a single moving receiver with an unknown signal period.
- We develop an SDP-based algorithm for the NLS problem, and design a fixed point iteration (FPI) method to improve the performance of the SDP algorithm.
- The proposed algorithm is extended to the case of receiver position errors.

The rest of this paper is organized as follows. Section II describes the pseudo-range measurement model, and derives the Cramér-Rao lower bounds (CRLB). In Section III, we first derive an SDP-based algorithm when receiver position are accurately known. Then, we develop an improved solution by FPI method. In Section IV, We extend the algorithm to address the receiver position uncertainties. Simulation results are presented in Section V to evaluate the estimation accuracy of the proposed algorithms and compare them with the CRLB.

Notation: Bold uppercase and bold lowercase letters denote matrices and vectors, respectively. $\mathbf{I}_m$ is the $m \times m$ identity matrix, $\mathbf{1}_m$ is the column vector of m ones, and $\mathbf{0}_{m,n}$ is the $m \times n$ zero matrix. $\|\cdot\|$ denotes the Euclidean distance, $\|\cdot\|_F$ denotes the Frobenius norm, and $[\cdot]^T$ denotes the transpose operation. For symmetric matrices $\mathbf{A}$ and $\mathbf{B}$, $\mathbf{A} \succeq \mathbf{B}$ means that $\mathbf{A} - \mathbf{B}$ is positive semidefinite.

II. TOA Measurements Model and CRLB

Consider a moving target at constant velocity transmitting periodic signal with an unknown period τ. Assuming the moving target begins to transmit periodic signal at t_0 and the unknown initial position of target at t_0 is $\mathbf{u}_0 = [x_0, y_0]^T$ (for simplicity, we consider the 2-D scenario, the extension to the 3-D case is straight-forward), and the moving receiver receives the signal waveform at t_1. The position of the moving receiver at t_1 is $\mathbf{s}_1 = [x_1, y_1]^T$ which is known, for example, from the GPS. After counting N waveforms, the receiver receives the new signal waveform at t_2, and the position of the moving receiver at t_2 is $\mathbf{s}_2 = [x_2, y_2]^T$. The rest can be done in the same manner, after counting $N(M-1)$ waveforms, the receiver receives the new waveform at t_M, and the position of the moving receiver at t_M is $\mathbf{s}_M = [x_M, y_M]^T$. For simplicity, we setting $\mathrm{T} = N\tau$ in the followings.

In Fig. 1, we present a diagram to illustrate the motion models and measurement models of the target and receiver. We can write the following expression (in this paper, we assume that the TOA is estimated, and our focus is using the estimated TOA to locate the position of the target) [5]:

$$t_i = t_0 + (i-1)\mathrm{T} + \frac{\|\mathbf{u}_{i-1} - \mathbf{s}_i\|}{c} + e_i, i = 1, 2, \ldots, M. \quad (1)$$

where c is the signal propagation speed, and e_i is the receiver TOA measurement noise at $\mathbf{s}_i$. In order to eliminate ambiguity, it is assumed that $\|\mathbf{u}_{i-1} - \mathbf{s}_i\| < \tau c, i = 1, \ldots, M$ [18].

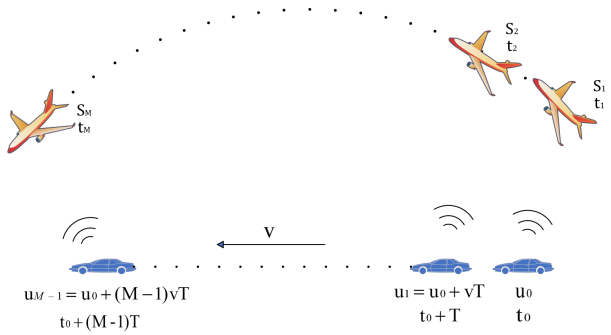

Fig. 1: The diagram of moving target at constant velocity localization using TOA measurements from single moving receiver. The plane denotes the single moving receiver, and the car denotes the moving target with constant velocity.

We assume that the target is moving with a constant velocity $\mathbf{v} = [v_x, v_y]^T$, then the target location at $t_0 + (i-1)\mathrm{T}$ can be expressed as

$$\mathbf{u}_{i-1} = \mathbf{u}_0 + (i-1)\mathrm{T}\mathbf{v}, i = 1, 2, \ldots, M. \quad (2)$$

Putting (2) into (1) and multiplying both sides by c yield

$$r_i = t_i c = t_0 c + (i-1)\mathrm{T}c + \|\mathbf{u}_0 + (i-1)\mathrm{T}\mathbf{v} - \mathbf{s}_i\| + n_i \quad (3)$$

where r_i is pseudo-range measurement, and $n_i = e_i c$. For ease of analysis, we assume that n_i is a zero-mean white Gaussian variable with variance σ_i^2.

From Eq. (3), we can write the non-linear least squares (NLS) problem:

$$\min_{\substack{\mathbf{u}_0, \mathbf{v}, \\ t_0, \mathrm{T}}} \sum_{i=1}^{M} \left(r_i - \|\mathbf{u}_0 + (i-1)\mathrm{T}\mathbf{v} - \mathbf{s}_i\| - t_0 c - (i-1)\mathrm{T}c\right)^2 \quad (4)$$

where $\mathbf{u}_0$, $\mathbf{v}$, t_0, and T are the optimization parameters. Since the above problem is highly nonlinear and nonconvex, a closed-form solution is hard to find. Exhaustive search in the solution space is directly, but its computational complexity is huge, making it impracticable to implement.

Given the TOA measurement model in (3), the performance of any unbiased estimate of $\boldsymbol{\zeta} = [\mathbf{u}_0^T, \mathbf{v}^T, t_0, \mathrm{T}]^T \in \mathbb{R}^{6\times 1}$ would be limited by the CRLB. The Fisher information matrix is calculated as [29]

$$\mathbf{I}(\boldsymbol{\zeta}) = \mathbf{H}(\boldsymbol{\zeta})^T \mathbf{Q} \mathbf{H}(\boldsymbol{\zeta}) \quad (5)$$

where $\mathbf{Q} = \mathrm{diag}([\sigma_1^{-2}, \sigma_2^{-2}, \ldots, \sigma_M^{-2}])$, and the i th row of $\mathbf{H}(\boldsymbol{\zeta}) \in \mathbb{R}^{M\times 6}$ is $[\frac{\left(\mathbf{u}_0+(i-1)\mathrm{T}\mathbf{v}-\mathbf{s}_i\right)^T}{\|\mathbf{u}_0+(i-1)\mathrm{T}\mathbf{v}-\mathbf{s}_i\|}, \frac{(i-1)\mathrm{T}\left(\mathbf{u}_0+(i-1)\mathrm{T}\mathbf{v}-\mathbf{s}_i\right)^T}{\|\mathbf{u}_0+(i-1)\mathrm{T}\mathbf{v}-\mathbf{s}_i\|}, c, (i-1)c + \frac{(i-1)\mathbf{v}^T\left(\mathbf{u}_0+(i-1)\mathrm{T}\mathbf{v}-\mathbf{s}_i\right)}{\|\mathbf{u}_0+(i-1)\mathrm{T}\mathbf{v}-\mathbf{s}_i\|}]$. As a result, the CRLB of $\mathbf{u}_0$, $\mathbf{v}$, t_0, and T are computed as

$$\mathrm{Var}(\mathbf{u}_0) \geq [\mathbf{I}^{-1}(\boldsymbol{\zeta})]_{1,1} + [\mathbf{I}^{-1}(\boldsymbol{\zeta})]_{2,2}, \quad (6a)$$

$$\mathrm{Var}(\mathbf{v}) \geq [\mathbf{I}^{-1}(\boldsymbol{\zeta})]_{3,3} + [\mathbf{I}^{-1}(\boldsymbol{\zeta})]_{4,4}, \quad (6b)$$

$$\mathrm{Var}(t_0) \geq [\mathbf{I}^{-1}(\boldsymbol{\zeta})]_{5,5}, \quad (6c)$$

$$\mathrm{Var}(\mathrm{T}) \geq [\mathbf{I}^{-1}(\boldsymbol{\zeta})]_{6,6}. \quad (6d)$$

III. Localization with Accurate Receiver's Positions

A. Original Solution By SDP

In this section, we describe how an SDP method can be used to solve the NLS problem in Eq. (4). Note that Eq. (4) can be expressed as the matrix-vector form

$$\min_{\mathbf{u}_0,\mathbf{v},\mathbf{d},t_0,\mathrm{T}} \ \|\mathbf{r}-\mathbf{d}-t_0c\mathbf{1}_M-\mathrm{T}c\mathbf{q}\|^2 \tag{7a}$$

$$\text{s. t. } d_i=\|\mathbf{u}_0+(i-1)\mathrm{T}\mathbf{v}-\mathbf{s}_i\|,\ i=1,2,\ldots,M. \tag{7b}$$

where $\mathbf{d}=[d_1,d_2,\ldots,d_M]^T$, $\mathbf{r}=[r_1,r_2,\ldots,r_M]^T$, $\mathbf{q}=[0,1,\ldots,M-1]^T$. Set $\mathbf{h}=[t_0,\mathrm{T}]^T\in\mathbb{R}^{2\times1}$, $\mathbf{F}=[\mathbf{1}_M,\mathbf{q}]\in\mathbb{R}^{M\times2}$, $\mathbf{f}_i=[1,i-1]^T\in\mathbb{R}^{2\times1}$, and $\mathbf{X}=[\mathbf{u}_0,\mathrm{T}\mathbf{v}]\in\mathbb{R}^{2\times2}$. Therefore, Eq. (7) can be expressed as

$$\min_{\mathbf{X},\mathbf{d},\mathbf{h}} \ \|\mathbf{r}-\mathbf{d}-c\mathbf{F}\mathbf{h}\|^2 \tag{8a}$$

$$\text{s. t. } d_i=\|\mathbf{X}\mathbf{f}_i-\mathbf{s}_i\| \tag{8b}$$

Instead of finding $\mathbf{X}$, $\mathbf{d}$, and $\mathbf{h}$ jointly, we find the optimum $\mathbf{h}$ as a dependent function of $\mathbf{d}$. Letting the gradient of the objective function in Eq. (8a) with respect to $\mathbf{h}$ to zero, then gives

$$-2c\mathbf{F}^T(\mathbf{r}-\mathbf{d}-c\mathbf{F}\mathbf{h})=\mathbf{0} \tag{9}$$

As a result, the optimum estimation of $\mathbf{h}$ is

$$\mathbf{h}=\frac{1}{c}(\mathbf{F}^T\mathbf{F})^{-1}\mathbf{F}^T(\mathbf{r}-\mathbf{d}) \tag{10}$$

Next, substituting the above $\mathbf{h}$ into Eq. (8) yields

$$\min_{\mathbf{X},\mathbf{d}} \ (\mathbf{r}-\mathbf{d})^T\mathbf{G}(\mathbf{r}-\mathbf{d}) \tag{11a}$$

$$\text{s. t. } d_i=\|\mathbf{X}\mathbf{f}_i-\mathbf{s}_i\|. \tag{11b}$$

where $\mathbf{G}=\mathbf{I}_M-\mathbf{F}(\mathbf{F}^T\mathbf{F})^{-1}\mathbf{F}^T$. It can be seen that (11a) is convex with respect to the unknown variable $\mathbf{d}$. However, (11b) is nonconvex with respect to the unknown variables $\mathbf{d}$ and $\mathbf{X}$. Next, we use the semidefinite positive relaxation (SDR) [30] techniques to relax Eq. (11).

Let $\mathbf{D}=\mathbf{d}\mathbf{d}^T$ and $\mathbf{Y}=\mathbf{X}^T\mathbf{X}$. The objective function in (11a) can be changed to

$$\mathrm{tr}(\mathbf{D}\mathbf{G})-2\mathbf{r}^T\mathbf{G}\mathbf{d}+\mathbf{r}^T\mathbf{G}\mathbf{r}. \tag{12}$$

And the non-convex constraints in Eq. (11b) can be relaxed to

$$\mathbf{D}_{i,i}=d_i^2=\mathrm{tr}(\mathbf{f}_i\mathbf{f}_i^T\mathbf{Y})-2\mathbf{f}_i^T\mathbf{X}^T\mathbf{s}_i+\mathbf{s}_i^T\mathbf{s}_i. \tag{13}$$

Finally, we obtain an SDP-based algorithm

$$\min_{\mathbf{d},\mathbf{D},\mathbf{X},\mathbf{Y}} \ \mathrm{tr}(\mathbf{D}\mathbf{G})-2\mathbf{r}^T\mathbf{G}\mathbf{d}+\mathbf{r}^T\mathbf{G}\mathbf{r} \tag{14a}$$

$$\text{s. t. } \mathbf{D}_{i,i}=\mathrm{tr}(\mathbf{f}_i\mathbf{f}_i^T\mathbf{Y})-2\mathbf{f}_i^T\mathbf{X}^T\mathbf{s}_i+\mathbf{s}_i^T\mathbf{s}_i, \tag{14b}$$

$$\begin{bmatrix}\mathbf{D} & \mathbf{d}\\ \mathbf{d}^T & 1\end{bmatrix}\succeq\mathbf{0}_{M+1,M+1}, \tag{14c}$$

$$\begin{bmatrix}\mathbf{Y} & \mathbf{X}^T\\ \mathbf{X} & \mathbf{I}_2\end{bmatrix}\succeq\mathbf{0}_{4,4}. \tag{14d}$$

After the above convex problem has been solved, we can obtain the estimation $\hat{\mathbf{X}}$, and then the parameters can be calculated as:

$$\hat{\mathbf{u}}_0=\hat{\mathbf{X}}(:,1) \tag{15a}$$

$$\hat{\mathbf{d}}_i=\left\|\hat{\mathbf{X}}\mathbf{f}_i-\mathbf{s}_i\right\|, \tag{15b}$$

$$\hat{\mathbf{h}}=\frac{1}{c}(\mathbf{F}^T\mathbf{F})^{-1}\mathbf{F}^T(\mathbf{r}-\hat{\mathbf{d}}), \tag{15c}$$

$$\hat{t}_0=\hat{\mathbf{h}}(\mathbf{1}), \tag{15d}$$

$$\hat{\mathrm{T}}=\hat{\mathbf{h}}(\mathbf{2}), \tag{15e}$$

$$\hat{\mathbf{v}}=\frac{\hat{\mathbf{X}}(:,2)}{\hat{\mathrm{T}}}. \tag{15f}$$

In the section of simulation, we also find that the SDP algorithm with second-order cone (SOC) constraints and penalty term still cannot reach the CRLB.

B. Improved Solution by FPI

Although the SDP-based algorithm in Eq. (14) can provide an estimate for the unknown parameter vector $\boldsymbol{\zeta}$, the estimate cannot reach the CRLB. This is due to the fact that the two rank constraints ($\mathrm{rank}(\mathbf{D})=1$, and $\mathrm{rank}(\mathbf{Y})=2$) are discarded and matrix $\mathbf{G}$ is singular [24], [31]. Next, we develop an FPI method to improve its solution. Actually, there also exist other methods that can improve the accuracy of the SDP-based algorithm, for example, Gauss-Newton method and SDP algorithm with second-order cone (SOC) constraints and penalty term [22]. However, the Gauss-Newton method has inferior performance due to its first-order approximation in the derivations [32]. And the SDP algorithm with second-order cone (SOC) constraints and penalty term is still sub-optimal as shown in the section of simulation results. As will be shown below, there is no first-order approximation in the derivations of the FPI. As a result, we choose the FPI algorithm to improve the accuracy of the SDP-based algorithm.

Let $\boldsymbol{\theta}=[\mathbf{u}_0^T,\mathrm{T}\mathbf{v}^T]^T\in\mathbb{R}^{4\times1}$, the optimization problem in Eq. (11) can be rewritten as:

$$\min_{\boldsymbol{\theta},\mathbf{d}} \ (\mathbf{r}-\mathbf{d})^T\mathbf{G}(\mathbf{r}-\mathbf{d}) \tag{16a}$$

$$s.t.\ d_i=\|\mathbf{P}_i\boldsymbol{\theta}-\mathbf{s}_i\|. \tag{16b}$$

where

$$\mathbf{P}_i=\begin{bmatrix}1 & 0 & i-1 & 0\\ 0 & 1 & 0 & i-1\end{bmatrix}. \tag{17}$$

Eq. (16) can also be written as the unconstrained optimization problem

$$\min_{\boldsymbol{\theta}}\sum_{i=1}^{M}\sum_{j=1}^{M}G_{ij}\big(r_i-\|\mathbf{P}_i\boldsymbol{\theta}-\mathbf{s}_i\|\big)\big(r_j-\|\mathbf{P}_j\boldsymbol{\theta}-\mathbf{s}_j\|\big) \tag{18}$$

Taking the derivative of the objective function in (18) with respect to $\boldsymbol{\theta}$, we obtain the gradient

$$\mathbf{g}_1=\sum_{i=1}^{M}\sum_{j=1}^{M}-2G_{ij}\big(r_i-\|\mathbf{P}_i\boldsymbol{\theta}-\mathbf{s}_i\|\big)\frac{\mathbf{P}_j^T(\mathbf{P}_j\boldsymbol{\theta}-\mathbf{s}_j)}{\|\mathbf{P}_j\boldsymbol{\theta}-\mathbf{s}_j\|} \tag{19}$$

where 2 is derived from the fact that $\mathbf{G}$ is a symmetric matrix. Letting $\mathbf{g}_1$ equal zero, we obtain

$$\boldsymbol{\theta} = f_1(\boldsymbol{\theta}) = (\sum_{i=1}^{M} G_{ii}\mathbf{P}_i^T\mathbf{P}_i)^{-1}\cdot \Big(\sum_{i=1}^{M} G_{ii}\mathbf{P}_i^T\big(\mathbf{s}_i + r_i\frac{\mathbf{P}_i\boldsymbol{\theta}-\mathbf{s}_i}{\|\mathbf{P}_i\boldsymbol{\theta}-\mathbf{s}_i\|}\big)+ \sum_{i=1}^{M}\sum_{j\neq i}^{M} G_{ij}\big(r_i - \|\mathbf{P}_i\boldsymbol{\theta}-\mathbf{s}_i\|\big)\frac{\mathbf{P}_j\boldsymbol{\theta}-\mathbf{s}_j}{\|\mathbf{P}_j\boldsymbol{\theta}-\mathbf{s}_j\|}\Big). \tag{20}$$

From Eq. (20), we developed an FPI method to update $\boldsymbol{\theta}$. We choose the solution from the SDP algorithm in Eq. (14) as the initial value, i.e., $\boldsymbol{\theta}_0 = [\hat{\mathbf{X}}(:,1)^T, \hat{\mathbf{X}}(:,2)^T]^T$, and $\boldsymbol{\theta}$ is updating as follows:

$$\boldsymbol{\theta}_k = f_1(\boldsymbol{\theta}_{k-1}). \tag{21}$$

A limit on the number of iterations, K_{max}, should be applied for practical scenarios. One proper criterion to stop the iteration is when the following condition is met:

$$\|\boldsymbol{\theta}_k - \boldsymbol{\theta}_{k-1}\| \leq \epsilon \tag{22}$$

where ϵ is a predetermined threshold. Unfortunately, the theoretical convergence proof of the FPI is difficult. Here, we provide a numerical simulation result to show the convergence of the FPI (the simulation settings are given in Section V). From Fig. 2, it can be seen that the estimation of $\boldsymbol{\theta}$ provided by the FPI is converging to the true $\boldsymbol{\theta}$ as the number of iterations increases.

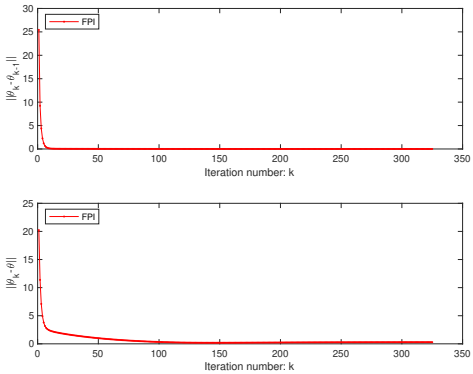

Fig. 2: $\|\boldsymbol{\theta}_k - \boldsymbol{\theta}_{k-1}\|$ and $\|\boldsymbol{\theta}_k - \boldsymbol{\theta}\|$ vs. iteration number k.

After $\hat{\boldsymbol{\theta}}$ has been obtained, the parameters can be obtained from

$$\hat{\mathbf{u}}_0 = \hat{\boldsymbol{\theta}}(1:2) \tag{23a}$$
$$\hat{\mathbf{d}}_i = \left\|\hat{\boldsymbol{\theta}}(1:2) - \mathbf{s}_i\right\|, \tag{23b}$$
$$\hat{\mathbf{h}} = \frac{1}{c}(\mathbf{F}^T\mathbf{F})^{-1}\mathbf{F}^T(\mathbf{r}-\hat{\mathbf{d}}), \tag{23c}$$
$$\hat{t}_0 = \hat{\mathbf{h}}(1), \tag{23d}$$
$$\hat{\mathrm{T}} = \hat{\mathbf{h}}(2), \tag{23e}$$
$$\hat{\mathbf{v}} = \frac{\hat{\boldsymbol{\theta}}(3:4)}{\hat{\mathrm{T}}}. \tag{23f}$$

IV. Localization with Non-accurate Receiver Positions

In the preceding development of Eqs. (14) and (20), we assume that the positions of receiver are accurate. However, in practice, the receiver positions may not be exact because of the imperfection of the navigation system. In this section, we will focus on developing robust localization algorithm in the presence of receiver position errors.

Under the condition of receiver position errors, the receiver positions can be expressed as [33]

$$\mathbf{a}_i = \mathbf{s}_i + \boldsymbol{\beta}_i,\ i = 1, 2, \ldots, M. \tag{24}$$

where $\boldsymbol{\beta}_i$ denotes the zero-mean white Gaussian vector with covariance $\delta_i^2\mathbf{I}_2$. Besides, n_i and $\boldsymbol{\beta}_i$ are mutually independent. We can write the NLS estimator:

$$\min_{\substack{\mathbf{u}_0,\mathbf{v},\\ \mathbf{s}_i,t_0,\mathrm{T}}} \sum_{i=1}^{M}(r_i - \|\mathbf{u}_0 + (i-1)\mathrm{T}\mathbf{v} - \mathbf{s}_i\| - t_0c - (i-1)\mathrm{T}c)^2 + \sum_{i=1}^{M}\|\mathbf{a}_i - \mathbf{s}_i\|^2 \tag{25}$$

where $\mathbf{u}_0$, $\mathbf{v}$, $\mathbf{s}_i$, t_0, and T are the optimization parameters.

Next, we will deduce the CRLB under receiver position errors. Set the unknown parameter vector as $\boldsymbol{\kappa} = [\mathbf{u}_0^T, \mathbf{v}^T, t_0, \mathrm{T}, \mathbf{s}_1^T, \mathbf{s}_2^T, \ldots, \mathbf{s}_M^T]^T \in \mathbb{R}^{(6+2M)\times 1}$. The Fisher information matrix of $\boldsymbol{\kappa}$ is calculated as [29]

$$\mathbf{I}(\boldsymbol{\kappa}) = \mathbf{I}_1(\boldsymbol{\kappa}) + \mathbf{I}_2(\boldsymbol{\kappa}) \tag{26}$$

where $\mathbf{I}_1(\boldsymbol{\kappa}) = \mathbf{P}_1(\boldsymbol{\kappa})\mathbf{Q}\mathbf{P}_1^T(\boldsymbol{\kappa})$, $\mathbf{I}_2(\boldsymbol{\kappa}) = \mathbf{P}_2(\boldsymbol{\kappa})\mathbf{W}\mathbf{P}_2^T(\boldsymbol{\kappa})$, $\mathbf{W} = \mathrm{diag}([\delta_1^{-2}, \delta_1^{-2}, \delta_2^{-2}, \delta_2^{-2}, \ldots, \delta_M^{-2}, \delta_M^{-2}])$,

$$\mathbf{P}_1(\boldsymbol{\kappa}) = \begin{bmatrix} \mathbf{H}(\boldsymbol{\zeta})^T \\ \mathbf{H}_0 \end{bmatrix} \tag{27}$$

$$\mathbf{H}_0 = \begin{bmatrix} -\frac{\mathbf{u}_0-\mathbf{s}_1}{\|\mathbf{u}_0-\mathbf{s}_1\|} & \mathbf{0}_{2,1} & \cdots & \mathbf{0}_{2,1} \\ \mathbf{0}_{2,1} & -\frac{\mathbf{u}_0+\mathrm{T}\mathbf{v}-\mathbf{s}_2}{\|\mathbf{u}_0+\mathrm{T}\mathbf{v}-\mathbf{s}_2\|} & \cdots & \mathbf{0}_{2,1} \\ \vdots & \vdots & \ddots & \vdots \\ \mathbf{0}_{2,1} & \mathbf{0}_{2,1} & \cdots & -\frac{\mathbf{u}_0+(M-1)\mathrm{T}\mathbf{v}-\mathbf{s}_M}{\|\mathbf{u}_0+(M-1)\mathrm{T}\mathbf{v}-\mathbf{s}_M\|} \end{bmatrix} \tag{28}$$

and

$$\mathbf{P}_2(\boldsymbol{\kappa}) = \begin{bmatrix} \mathbf{0}_{2,2} & \mathbf{0}_{2,2} & \cdots & \mathbf{0}_{2,2} \\ \mathbf{0}_{2,2} & \mathbf{0}_{2,2} & \cdots & \mathbf{0}_{2,2} \\ \mathbf{0}_{2,2} & \mathbf{0}_{2,2} & \cdots & \mathbf{0}_{2,2} \\ \mathbf{I}_2 & \mathbf{0}_{2,2} & \cdots & \mathbf{0}_{2,2} \\ \mathbf{0}_{2,2} & \mathbf{I}_2 & \cdots & \mathbf{0}_{2,2} \\ \vdots & \vdots & \ddots & \vdots \\ \mathbf{0}_{2,2} & \mathbf{0}_{2,2} & \cdots & \mathbf{I}_2 \end{bmatrix}. \tag{29}$$

As a result, the CRLB of $\mathbf{u}_0$, $\mathbf{v}$, t_0, and T are computed as

$$\mathrm{Var}(\mathbf{u}_0) \geq [\mathbf{I}^{-1}(\boldsymbol{\kappa})]_{1,1} + [\mathbf{I}^{-1}(\boldsymbol{\kappa})]_{2,2}, \tag{30a}$$
$$\mathrm{Var}(\mathbf{v}) \geq [\mathbf{I}^{-1}(\boldsymbol{\kappa})]_{3,3} + [\mathbf{I}^{-1}(\boldsymbol{\kappa})]_{4,4}, \tag{30b}$$
$$\mathrm{Var}(t_0) \geq [\mathbf{I}^{-1}(\boldsymbol{\kappa})]_{5,5}, \tag{30c}$$
$$\mathrm{Var}(\mathrm{T}) \geq [\mathbf{I}^{-1}(\boldsymbol{\kappa})]_{6,6}. \tag{30d}$$

A. Original Solution By SDP

Using the result from Eq. (11), the NLS problem in Eq. (25) can be written in the matrix-vector form

$$\min_{\mathbf{X},\mathbf{d}} \ (\mathbf{r}-\mathbf{d})^T\mathbf{G}(\mathbf{r}-\mathbf{d}) + \|(\mathbf{A}-\mathbf{X}(:,3:M+2))\|_F^2 \quad (31a)$$

$$s.t.\ d_i = \|\mathbf{X}\mathbf{q}_i\|, \ i=1,2,\ldots,M. \quad (31b)$$

where $\mathbf{A} = [\mathbf{a}_1,\mathbf{a}_2,\ldots,\mathbf{a}_M] \in \mathbb{R}^{2\times M}$, $\mathbf{X} = [\mathbf{u}_0, \mathrm{T}\mathbf{v}, \mathbf{s}_1, \mathbf{s}_2, \ldots, \mathbf{s}_M] \in \mathbb{R}^{2\times(M+2)}$, $\mathbf{q}_i = [1, i-1, \mathbf{0}_{1,i-1}, -1, \mathbf{0}_{1,M-i}]^T \in \mathbb{R}^{(M+2)\times 1}$.

Similar to the derivation of Eq. (14), we can obtain an SDP-based algorithm with sensor position errors

$$\min_{\mathbf{d},\mathbf{D},\mathbf{X},\mathbf{Y}} \mathrm{tr}(\mathbf{D}\mathbf{G}) - 2\mathbf{r}^T\mathbf{G}\mathbf{d} - 2\mathrm{tr}(\mathbf{A}^T\mathbf{X}(:,3:M+2)) + \mathrm{tr}(\mathbf{Y}(3:M+2,3:M+2)) \quad (32a)$$

$$\text{s. t. } \mathbf{D}_{i,i} = \mathrm{tr}(\mathbf{q}_i\mathbf{q}_i^T\mathbf{Y}), \quad (32b)$$

$$\begin{bmatrix}\mathbf{D} & \mathbf{d}\\ \mathbf{d}^T & 1\end{bmatrix} \succeq \mathbf{0}_{M+1,M+1}, \quad (32c)$$

$$\begin{bmatrix}\mathbf{Y} & \mathbf{X}^T\\ \mathbf{X} & \mathbf{I}_2\end{bmatrix} \succeq \mathbf{0}_{M+4,M+4}. \quad (32d)$$

After the above convex problem has been solved, we can obtain the estimation $\hat{\mathbf{X}}$, and then the parameters can be calculated as:

$$\hat{\mathbf{u}_0} = \hat{\mathbf{X}}(:,1) \quad (33a)$$

$$\hat{\mathbf{d}}_i = \left\|\hat{\mathbf{X}}\mathbf{q}_i\right\|, \quad (33b)$$

$$\hat{\mathbf{h}} = \frac{1}{c}(\mathbf{F}^T\mathbf{F})^{-1}\mathbf{F}^T(\mathbf{r}-\hat{\mathbf{d}}), \quad (33c)$$

$$\hat{t}_0 = \hat{\mathbf{h}}(1), \quad (33d)$$

$$\hat{\mathrm{T}} = \hat{\mathbf{h}}(2), \quad (33e)$$

$$\hat{\mathbf{v}} = \frac{\hat{\mathbf{X}}(:,2)}{\hat{\mathrm{T}}}. \quad (33f)$$

B. Improved Solution by FPI

The estimates from the above SDP algorithm in Eq. (32) also cannot attain the corresponding CRLB. In order to get a better solution, an FPI algorithm is attached to the SDP estimation. Next, we will show how to develop the FPI algorithm. The optimization problem in Eq. (31) can be rewritten as:

$$\min_{\boldsymbol{\theta},\mathbf{d}} \ (\mathbf{r}-\mathbf{d})^T\mathbf{G}(\mathbf{r}-\mathbf{d}) + \|\mathbf{a}-\mathbf{B}\boldsymbol{\theta}\|^2 \quad (34a)$$

$$s.t.\ d_i = \|\mathbf{R}_i\boldsymbol{\theta}\|. \quad (34b)$$

where $\boldsymbol{\theta} = [\mathbf{u}_0^T, \mathrm{T}\mathbf{v}^T, \mathbf{s}_1^T, \mathbf{s}_2^T, \ldots, \mathbf{s}_M^T]^T \in \mathbb{R}^{(4+2M)\times 1}$, $\mathbf{a} = [\mathbf{a}_1^T, \mathbf{a}_2^T, \ldots, \mathbf{a}_M^T]^T \in \mathbb{R}^{2M\times 1}$, $\mathbf{R}_i = [\mathbf{P}_i, \mathbf{0}_{2,2i-2}, -\mathbf{I}_2, \mathbf{0}_{2,2M-2i}] \in \mathbb{R}^{2\times(4+2M)}$, and $\mathbf{B} = [\mathbf{0}_{2M,4}, \mathbf{I}_{2M}] \in \mathbb{R}^{2M\times(4+2M)}$.

Optimization problem in Eq. (34) can also be written as the form of unconstrained

$$\min_{\boldsymbol{\theta}} \sum_{i=1}^{M}\sum_{j=1}^{M} G_{ij}\big(r_i - \|\mathbf{R}_i\boldsymbol{\theta}\|\big)\big(r_j - \|\mathbf{R}_j\boldsymbol{\theta}\|\big) + \sum_{i=1}^{2M}(a_i - \mathbf{b}_i\boldsymbol{\theta})^2 \quad (35)$$

where $\mathbf{b}_i$ is the ith row vector of matrix $\mathbf{B}$, and a_i is the ith entry of vector $\mathbf{a}$. Taking the derivative of the objective function in (35) with $\boldsymbol{\theta}$, we obtain

$$\mathbf{g}_2 = \sum_{i=1}^{M}\sum_{j=1}^{M} -2G_{ij}\big(r_i - \|\mathbf{R}_i\boldsymbol{\theta}\|\big)\frac{\mathbf{R}_j^T\mathbf{R}_j\boldsymbol{\theta}}{\|\mathbf{R}_j\boldsymbol{\theta}\|} + \sum_{i=1}^{2M} -2\mathbf{b}_i^T(a_i - \mathbf{b}_i\boldsymbol{\theta}) \quad (36)$$

Letting $\mathbf{g}_2$ equal zero, we obtain

$$\boldsymbol{\theta} = f_2(\boldsymbol{\theta}) = \Big(\sum_{i=1}^{M} G_{ii}\mathbf{R}_i^T\mathbf{R}_i + \sum_{i=1}^{2M}\mathbf{b}_i^T\mathbf{b}_i\Big)^{-1}\cdot \Big(\sum_{i=1}^{M} G_{ii}r_i\mathbf{R}_i^T\frac{\mathbf{R}_i\boldsymbol{\theta}}{\|\mathbf{R}_i\boldsymbol{\theta}\|} + \sum_{i=1}^{2M} a_i\mathbf{b}_i^T + \sum_{i=1}^{M}\sum_{j\neq i}^{M} G_{ij}\big(r_i - \|\mathbf{R}_i\boldsymbol{\theta}\|\big)\mathbf{R}_j^T\frac{\mathbf{R}_j\boldsymbol{\theta}}{\|\mathbf{R}_j\boldsymbol{\theta}\|}\Big) \quad (37)$$

From Eq. (37), we developed an FPI method to estimate the parameter vector $\boldsymbol{\theta}$. We choose the solution from the SDP algorithm in Eq. (32) as the initial value, i.e., $\boldsymbol{\theta}_0 = [\hat{\mathbf{X}}(:,1)^T, \hat{\mathbf{X}}(:,2)^T, \ldots, \hat{\mathbf{X}}(:,M+2)^T]^T$, and $\boldsymbol{\theta}$ is updating as follows:

$$\boldsymbol{\theta}_k = f_2(\boldsymbol{\theta}_{k-1}) \quad (38)$$

The criterion to stop the iteration is same to Eq. (22).

V. Simulation Results

In this section, we conduct several numerical simulations to show the performance of proposed algorithms when receiver positions are accurate and non-accuratre, respectively. The initial values from (14) and (32) are labelled as "SDP", the improved solutions from (20) and (37) are labelled as "SDP+FPI", and the SDP algorithm with SOC constraints and penalty term is labeled as "SDP+SOC+Penalty" [1] [22]. The SDP-based algorithms are implemented by the CVX toolbox [34] using SeDuMi as a solver [35], and the precision is set to best[2]. The parameters of the stop criterion for FPI algorithm are: $K_{max} = 1000$, $\epsilon = 10^{-4}$. The root-mean-square errors (RMSEs) are calculated as follows:

$$\mathrm{RMSE}(\mathbf{u}_0) = \sqrt{\frac{1}{M_c}\sum_{j=1}^{M_c}\|\mathbf{u}_0 - \hat{\mathbf{u}}_0^j\|^2}, \quad (39a)$$

$$\mathrm{RMSE}(\mathbf{v}) = \sqrt{\frac{1}{M_c}\sum_{j=1}^{M_c}\|\mathbf{v} - \hat{\mathbf{v}}^j\|^2}, \quad (39b)$$

[1]The "SDP+SOC+Penalty" algorithm has two difference compared with the "SDP" algorithm: 1) the penalty term $\eta\mathrm{tr}(\mathbf{D})$ in objective function; 2) the SOC constraints. It is worth noting that the SOC constraints have two versions, $\|\mathbf{X}\mathbf{f}_i - \mathbf{s}_i\| \le d_i$ when receiver's positions are accurate, and $\|\mathbf{X}\mathbf{q}_i\| \le d_i$ when receiver's positions are non-accurate. In the following simulations, $\eta = 10^{-7}$.

[2]In the numerical simulations, scaling technique is used for the two SDP based algorithms to avoid the problem of inaccurate results induced from large numerical value. $\mathbf{r}$, $\mathbf{s}_i$ and $\mathbf{a}_i$ are shrunk to the values of one in a thousand.

This article has been accepted for publication in IEEE Open Journal of Signal Processing. This is the author's version which has not been fully edited and content may change prior to final publication. Citation information: DOI 10.1109/OJSP.2023.3338111

TABLE I: The average running time [s] of the considered algorithms with the two scenarios, CPU: i7-10700, 2.9 GHz.

Algorithms \ Scenarios	1	2
SDP	0.2586	0.2542
SDP+FPI	0.3764	0.5045
SDP+SOC+Penalty	0.3837	0.3781

$$\mathrm{RMSE}(t_0) = \sqrt{\frac{1}{M_c}\sum_{j=1}^{M_c}(t_0 - \hat{t}_0^j)^2}, \tag{39c}$$

$$\mathrm{RMSE}(\mathrm{T}) = \sqrt{\frac{1}{M_c}\sum_{j=1}^{M_c}(\mathrm{T} - \hat{\mathrm{T}}^j)^2}, \tag{39d}$$

where M_c is the number of Monte Carlo runs, $\hat{\mathbf{u}}_0^j$, $\hat{\mathbf{v}}^j$, $\hat{t}_0^j$, and $\hat{\mathrm{T}}^j$ are respectively, the estimates of $\mathbf{u}_0$, $\mathbf{v}$, t_0, and T in the j-th run. In the following simulations, we set $M_c = 2000$. The receiver is moving in a 2-dimensional plane, the signal period τ is set to $1ms$, and the number N between two TOA measurements is set to 60000, so the corresponding $\mathrm{T} = N \times \tau$ is $60s$. The starting transmission time t_0 is drawn from a uniform distribution $[0, 1]s$. The initial position of target is $\mathbf{u}_0 = [300, 2600]^T m$, and the velocity of target is $\mathbf{v} = [15, 25]^T m/s$. The moving trajectory of receiver is a count-clockwise circle, and its center and radius are $[0, 0]^T m$ and $L = 10000m$, respectively. The speed of the moving receiver is $w = 200m/s$, and the number of TOA measurements is $M = 10$. The positions of the receiver at different measurement time are:

$$x_i = L\cos(\frac{w\mathrm{T}(i-1)}{L}), i = 1, 2, \ldots, M \tag{40a}$$

$$y_i = L\sin(\frac{w\mathrm{T}(i-1)}{L}), i = 1, 2, \ldots, M. \tag{40b}$$

The trajectory of the receiver and target is depicted in Fig. 3. The variances of noise are assumed to be identical, i.e., $\sigma_i^2 = \sigma^2, \delta_i^2 = \delta^2,\ i = 1, 2, \ldots, M$. δ is set to $0.3m$ in the presence of receiver position uncertainties.

Fig. 4 to Fig. 7 are, respectively, the RMSE results of $\mathbf{u}_0$, $\mathbf{v}$, t_0, and T as the TOA measurement noise variance increase when receiver's positions are accurate. From these figures, we can obtain the following observations: 1) the "SDP" algorithm cannot reach the CRLB; 2) the "SDP+SOC+Penalty" algorithm has better performance than the "SDP" algorithm, but it still cannot reach the CRLB; 3) the "SDP+FPI" algorithm attains the CRLB. This observation validates that the FPI method converges on the global minimum.

Fig. 8 to Fig. 11 are the four RMSE results obtained in the presence of receiver position errors. The observation results are similar to the former case. Besides, in Table I, the average running time of the three algorithms are provided. From the table, it is worth noting that the proposed "SDP+FPI" algorithm costs more running time in the case of receiver position errors. This is due to the fact that the calculation of the FPI is more complicated in this case.

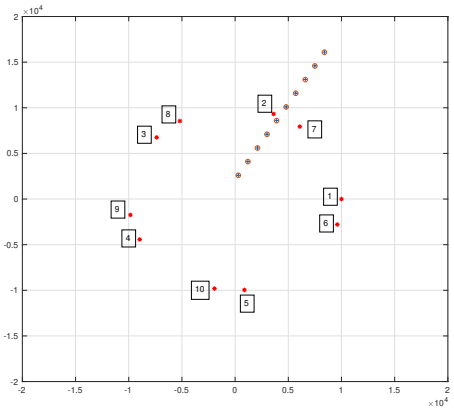

Fig. 3: Performance of the proposed solution when receiver's positions are accurate. The red stars denote the positions of the receiver, the open circles are the true positions of the moving target, and the crosses denote the estimates from the proposed algorithm.

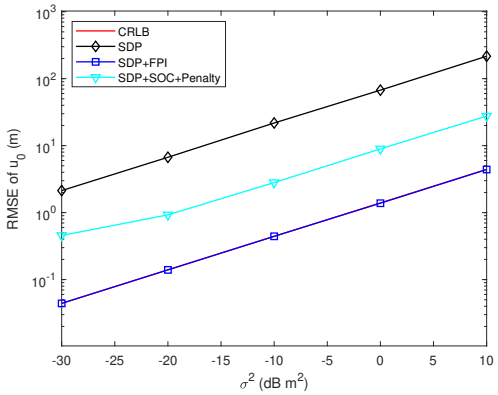

Fig. 4: RMSE of $\mathbf{u}_0$ vs. σ^2.

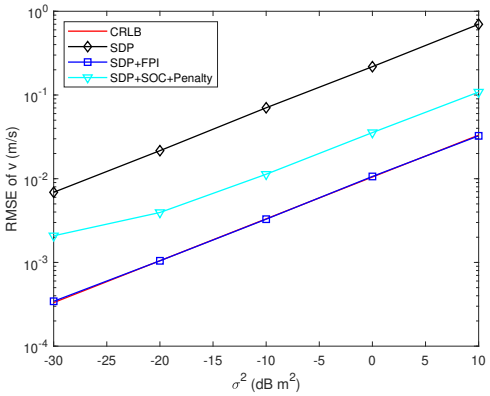

Fig. 5: RMSE of $\mathbf{v}$ vs. σ^2.

This article has been accepted for publication in IEEE Open Journal of Signal Processing. This is the author's version which has not been fully edited and content may change prior to final publication. Citation information: DOI 10.1109/OJSP.2023.3338111

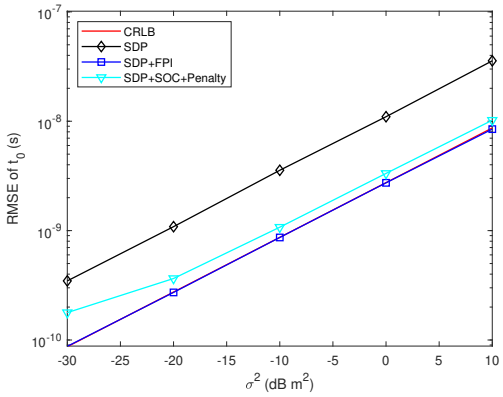

Fig. 6: RMSE of t_0 vs. σ^2.

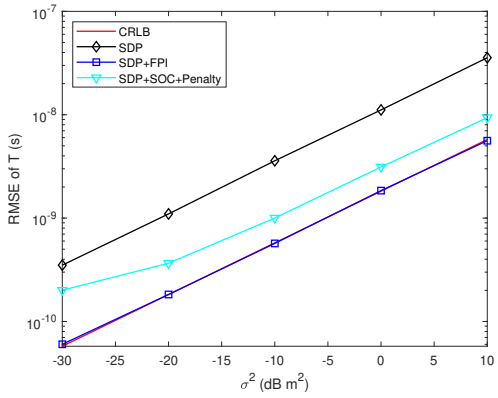

Fig. 7: RMSE of T vs. σ^2.

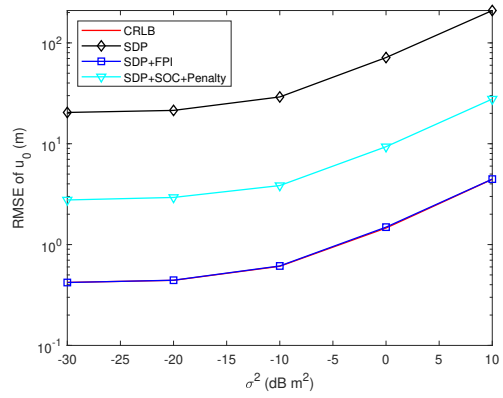

Fig. 8: RMSE of $\mathbf{u}_0$ vs. σ^2 with $\delta = 0.3m$.

VI. Conclusions

In this paper, we have investigated the problem of moving target at constant velocity localization by using a single moving receiver. We derived an SDP-based algorithm to provide a rough estimation of unknown parameters, and then an FPI method was derived to improve the performance of the SDP algorithm. The algorithm is also extended to take receiver position uncertainties into consideration. Simulation results have shown that the proposed algorithms can attain the CRLB.

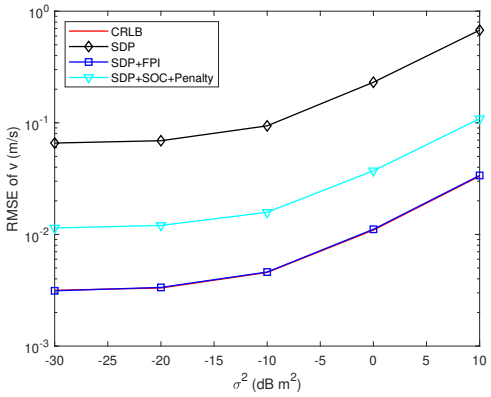

Fig. 9: RMSE of $\mathbf{v}$ vs. σ^2 with $\delta = 0.3m$.

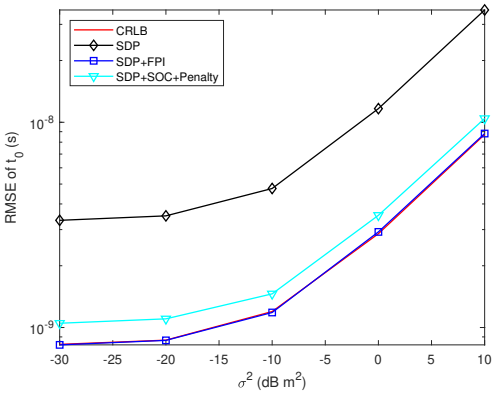

Fig. 10: RMSE of t_0 vs. σ^2 with $\delta = 0.3m$.

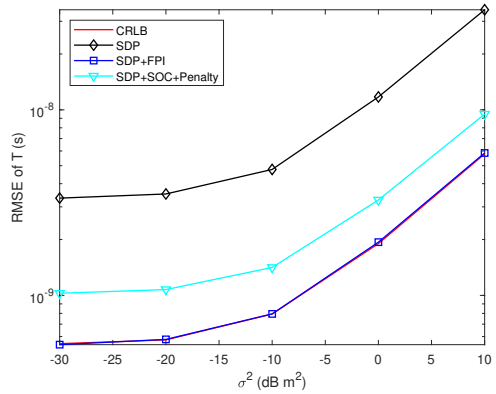

Fig. 11: RMSE of T vs. σ^2 with $\delta = 0.3m$.

Acknowledgment

The authors would like to thank the Associate Editor and anonymous reviewers for their careful review and constructive comments. This work was supported in part by STU Scientific Research Foundation for Talents under Grant NTF19036.

References

[1] K. C. Ho, X. Lu, and L. Kovavisaruch, "Source localization using TDOA and FDOA measurements in the presence of receiver location errors: Analysis and solution," *IEEE Trans. Signal Process.*, vol. 55, no. 2, pp. 684–696, 2007.

[2] Y. Zou and Q. Wan, "Moving target localization in noncoherent distributed mimo radar systems using range and range rate measurements," in *Asia-Pacific Signal and Information Processing Association Annual Summit and Conference*, 2016, pp. 1–6.

[3] M. Z. Win, Y. Shen, and W. Dai, "A theoretical foundation of network localization and navigation," *Proceedings of the IEEE*, vol. 106, no. 7, pp. 1136–1165, 2018.

[4] J. Yan, H. Ban, X. Luo, H. Zhao, and X. Guan, "Joint localization and tracking design for AUV with asynchronous clocks and state disturbances," *IEEE Trans. Veh. Technol.*, vol. 68, no. 5, pp. 4707–4720, 2019.

[5] Y. Zou and H. Liu, "A simple and efficient iterative method for TOA localization," in *IEEE International Conference on Acoustics, Speech and Signal Processing*, 2020, pp. 4881–4884.

[6] A. Beck, P. Stoica, and J. Li, "Exact and approximate solutions of source localization problems," *IEEE Trans. Signal Process.*, vol. 56, no. 5, pp. 1770–1778, 2008.

[7] E. Alamdari, F. Behnia, and R. Amiri, "Conical localization from angle measurements: An approximate convex solution," *IEEE Sensors Lett.*, vol. 6, no. 5, pp. 1–4, 2022.

[8] Y. Zou and H. Liu, "Semidefinite programming methods for alleviating clock synchronization bias and sensor position errors in TDOA localization," *IEEE Signal Process. Lett.*, vol. 27, pp. 241–245, 2020.

[9] J. Yin, Q. Wan, S. Yang, and K. C. Ho, "A simple and accurate TDOA-AOA localization method using two stations," *IEEE Signal Process. Lett.*, vol. 23, no. 1, pp. 144–148, 2016.

[10] A. O'connor, P. Setlur, and N. Devroye, "Single-sensor RF emitter localization based on multipath exploitation," *IEEE Trans. Aerosp. Electron. Syst.*, vol. 51, no. 3, pp. 1635–1651, 2015.

[11] F. Quitin, Z. Madadi, and W. P. Tay, "RF transmitter geolocation based on signal periodicity: Concept and implementation," in *IEEE International Conference on Communications*, 2015, pp. 4593–4598.

[12] S. Zhang, Z. Huang, and J. He, "A single sensor passive localization algorithm using second difference of time delay," in *IEEE Global Conference on Signal and Information Processing*, 2017, pp. 328–332.

[13] X. Feng, Z. Huang, and J. He, "A 1-d search approach for single sensor passive localization based on signal periodicity," *IEEE Commun. Lett.*, vol. 25, no. 7, pp. 2221–2225, 2021.

[14] K. Doğançay, "Bearings-only target localization using total least squares," *Signal Process.*, vol. 85, no. 9, pp. 1695–1710, 2005.

[15] B. Lee, Y. Chan, F. Chan, H.-J. Du, and F. A. Dilkes, "Doppler frequency geolocation of uncooperative radars," in *IEEE Military Communications Conference*, 2007, pp. 1–6.

[16] A. Amar and A. J. Weiss, "Localization of narrowband radio emitters based on doppler frequency shifts," *IEEE Trans. Signal Process.*, vol. 56, no. 11, pp. 5500–5508, 2008.

[17] N. H. Nguyen and K. Doğançay, "Single-platform passive emitter localization with bearing and doppler-shift measurements using pseudolinear estimation techniques," *Signal Process.*, vol. 125, pp. 336–348, 2016.

[18] E. Tzoreff, B. Z. Bobrovsky, and A. J. Weiss, "Single receiver emitter geolocation based on signal periodicity with oscillator instability," *IEEE Trans. Signal Process.*, vol. 62, no. 6, pp. 1377–1385, 2014.

[19] Z. Madadi, F. Quitin, and W. P. Tay, "Periodic RF transmitter geolocation using a mobile receiver," in *IEEE International Conference on Acoustics, Speech and Signal Processing*, 2015, pp. 2584–2588.

[20] E. Tzoreff and A. J. Weiss, "Single sensor path design for best emitter localization via convex optimization," *IEEE Trans. Wireless Commun.*, vol. 16, no. 2, pp. 939–951, 2016.

[21] Y. Liu, F. Guo, L. Yang, and W. Jiang, "Source localization using a moving receiver and noisy TOA measurements," *Signal Process.*, vol. 119, pp. 185–189, 2016.

[22] Y. Zou and Q. Wan, "Emitter source localization using time-of-arrival measurements from single moving receiver," in *IEEE International Conference on Acoustics, Speech and Signal Processing*, 2017, pp. 3444–3448.

[23] R. Kaune, "Accuracy studies for TDOA and TOA localization," in *International Conference on Information Fusion*, 2012, pp. 408–415.

[24] Y. Zou and Q. Wan, "Asynchronous time-of-arrival-based source localization with sensor position uncertainties," *IEEE Commun. Lett.*, vol. 20, no. 9, pp. 1860–1863, 2016.

[25] X. Ma, B. Hao, H. Zhang, and P. Wan, "Semidefinite relaxation for source localization by TOA in unsynchronized networks," *IEEE Signal Process. Lett.*, vol. 29, pp. 622–626, 2022.

[26] X. R. Li and V. P. Jilkov, "Survey of maneuvering target tracking. part i. dynamic models," *IEEE Trans. Aerosp. Electron. Syst.*, vol. 39, no. 4, pp. 1333–1364, 2003.

[27] F. Xu, J. Wang, D. Zhu, and Q. Tu, "Speckle noise reduction technique for lidar echo signal based on self-adaptive pulse-matching independent component analysis," *Optics and Lasers in Engineering*, vol. 103, pp. 92–99, 2018.

[28] W. Lu, J. Xie, H. Wang, and C. Sheng, "Parameterized time-frequency analysis to separate multi-radar signals," *Journal of Systems Engineering and Electronics*, vol. 28, no. 3, pp. 493–502, 2017.

[29] S. M. Kay, *Fundamentals of statistical signal processing, volume I: estimation theory*. Prentice Hall, 1993.

[30] S. Boyd and L. Vandenberghe, *Convex optimization*. Cambridge university press, 2004.

[31] E. Xu, Z. Ding, and S. Dasgupta, "Source localization in wireless sensor networks from signal time-of-arrival measurements," *IEEE Trans. Signal Process.*, vol. 59, no. 6, pp. 2887–2897, June 2011.

[32] Y. Zou, J. Fan, L. Wu, and H. Liu, "Fixed point iteration based algorithm for asynchronous TOA-based source localization," *Sensors*, vol. 22, no. 18, p. 6871, 2022.

[33] Y. Zou, H. Liu, X. Wei, and Q. Wan, "Semidefinite programming methods for alleviating sensor position error in TDOA localization," *IEEE Access*, vol. 5, pp. 23 111–23 120, 2017.

[34] M. Grant and S. Boyd, "Cvx: Matlab software for disciplined convex programming, version 1.21," http://cvxr.com/cvx, May 2010.

[35] J. F. Sturm, "Using sedumi 1.02, a matlab toolbox for optimization over symmetric cones," *Optimization Methods and Software*, vol. 11, no. 1-4, pp. 625–653, Mar. 1999.

Yanbin Zou (S'13-M'19) received the B. S. degree in electronic and information engineering from Hebei Normal University of Science and Technology in 2011, and the Ph.D. degree in signal and information processing from University of Electronic Science and Technology of China in 2018. He is currently an assistant professor with the Department of Electronic Engineering, Shantou University, Shantou, China. His research interests include source localization and array signal processing.

Jingna Fan received the B.S. degree in electronic and information engineering from Beijing Institute of Technology, Zhuhai in 2020. She is currently a master student with the Department of Electronic Engineering, Shantou University, Shantou, China. Her research include source localization and convex optimization.

Zekai Zhang received the B.S. degree in automation engineering from Qingdao University, Qingdao in 2021. He is currently a master student with the Department of Electronic Engineering, Shantou University, Shantou, China. His research include source localization and convex optimization.